International Journal of Electrical, Electronic and Communication Sciences
ISSN: 2517-9438
Vol:3, No:4, 2009

Effect of Channel Estimation on Capacity of MIMO System Employing Circular or Linear Receiving Array Antennas

Xia Liu and Marek E. Bialkowski

***Abstract*—**This paper reports on investigations into capacity of a Multiple Input Multiple Output (MIMO) wireless communication system employing a uniform linear array (ULA) at the transmitter and either a uniform linear array (ULA) or a uniform circular array (UCA) antenna at the receiver. The transmitter is assumed to be surrounded by scattering objects while the receiver is postulated to be free from scattering objects. The Laplacian distribution of angle of arrival (AOA) of a signal reaching the receiver is postulated. Calculations of the MIMO system capacity are performed for two cases without and with the channel estimation errors. For estimating the MIMO channel, the scaled least square (SLS) and minimum mean square error (MMSE) methods are considered.

***Keywords*—**MIMO, channel capacity, channel estimation, ULA, UCA, spatial correlation

I. Introduction

IN recent years, there has been a growing interest in the communication research community in the signal transmission technique employing multiple element antennas both at the transmitter and receiver sides of a wireless communication system. The reason is that it can significantly improve the transmission quality in terms of data throughput (capacity) and coverage area without the need for extra operational frequency bandwidth. Known as the multiple-input multiple-output (MIMO) technique, it is one of the promising techniques for the next generation of mobile communications. For its physical implementation, the MIMO technique frequently assumes uniform linear arrays (ULA) at both the transmitter and receiver ends of a wireless communication system. However, to obtain operation with larger angular views, uniform circular arrays (UCA) and their alikes such as triangular, square, pentagonal or hexagonal arrays are also considered. It can be expected that different configurations of antenna arrays will result in different spatial correlations of transmitted/received signals and thus they will influence in a different way channel properties between transmitter and receiver. These, in turn, will affect in a different way the accuracy of channel estimation and the overall MIMO system capacity. This problem has been addressed in some recent works on MIMO. For example, in [1], the bit error rate (BER) performance of ULA and UCA is investigated under the assumption of a truncated Gaussian angle of arrival (AOA) distribution. In [2], the accuracy performance of MMSE channel estimation for UCA is presented under different spatial correlation conditions.

It has to be noted that most of the works on MIMO capacity assume that an accurate Channel State Information (CSI) is known to the receiver [3-6]. However, in actual systems CSI has to be estimated using a suitable channel estimation method. The methods based on the use of training sequences, known as the training-based channel estimation methods, are the most popular. It has been shown in [7], [8] that the accuracy of the training-based estimation methods is influenced by the transmitted signal power to noise ratio in the training mode and a number of antenna elements at the transmitter and receiver. In particular, it has been proved in [2], [7] and [8] that the performance of the training-based estimation methods based on scaled least square (SLS) and minimum mean square error (MMSE) algorithms is affected by spatial correlation. These findings indicate that the determination of MIMO channel capacity has to take into account imprecise knowledge of CSI that is available from the channel estimation procedure.

In this paper, calculations of the MIMO system capacity are performed for the two cases without and with the channel estimation errors. For channel estimation the SLS and MMSE estimation methods are considered. In the undertaken investigations it is assumed that the receiver employs either ULA or UCA antennas while the transmitter uses only ULA. Also assumed is that the transmitter is surrounded by scattering objects while the receiver is free from scatterers. To determine the antenna array spatial correlation pattern, a Laplacian distribution for the angle of arrival (AOA), which provides a good agreement with the measured data [9], is postulated.

II. System Model

A. System configuration and spatial correlations

Figure 1 shows the configuration of the investigated MIMO system. The case of 4x4 MIMO is considered.

X. Liu is with school of ITEE, the University of Queensland, St, Lucia Campus, QLD4072, Australia (phone: +61 7 33658308; e-mail: xialiu@ itee.uq.edu.au).

M. E. Bialkowski is with school of ITEE, the University of Queensland, St, Lucia Campus, QLD4072, Australia (e-mail: meb@ itee.uq.edu.au).

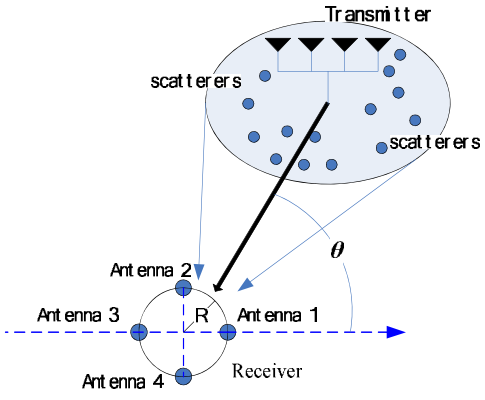

A. UCA

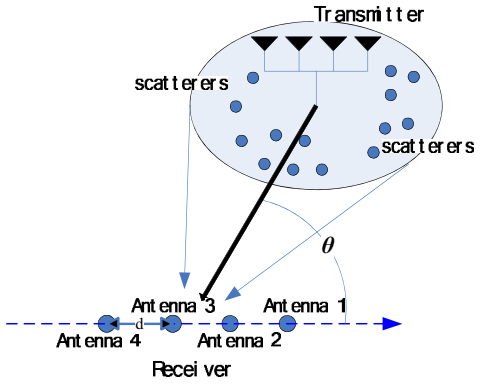

B. ULA

Fig. 1 4-element UCA and ULA

The transmitter is assumed to be equipped with a ULA antenna surrounded by scattering objects that are uniformly distributed in a circle. Antenna elements in the array have an omnidirectional radiation pattern in the azimuth plane. The considered case represents a mobile station operating close to the ground where many surrounding obstacles are expected. In turn, the receiver is assumed to be equipped with either ULA or UCA of omnidirectional antenna elements free from any surrounding obstacles. This configuration can represent a base station with antennas located high above the ground where there are no scattering objects.

In Figure 1, θ stands for the central AOA which is determined by the physical position of dominant scatterers with respect to the receiving antenna array. Assuming that the AOA follows the Laplacian distribution, the mathematical expressions for the real and imaginary parts of spatial correlation between the *m*-th and *n*-th antenna for the case of UCA receiving antenna are given as [9]:

$$\mathrm{Re}\{Rr(m,n)\} = J_0(Z_c) + 2\sum_{k=1}^{\infty} \frac{a^2(1-e^{-a\pi})}{a^2+4k^2} J_{2k}(Z_c)\cos[2k(\theta+\alpha)] \quad (1)$$

$$\mathrm{Im}\{Rr(m,n)\} = 4C_l \sum_{k=0}^{\infty} \frac{a^2(1-e^{-a\pi})}{a^2+(2k+1)^2} \cdot J_{2k+1}(Z_c)\sin[(2k+1)(\theta+\alpha)] \quad (2)$$

where C_l is a normalizing constant given as [9]:

$$C_l = \frac{a}{2(1-e^{-a\pi})} \quad (3)$$

with *a* representing a decay factor related to the angle spread (AS). When *a* increases the angle spread decreases. $J_n(.)$ is an *n*-th order Bessel function of the first kind. Z_c is related to the antenna spacing and α is the relative angle between the *m*-th and *n*-th antenna. If we let

$$K1 = 2\pi \frac{R}{\lambda}[\cos(\phi_m) - \cos(\phi_n)] \quad (4)$$

$$K2 = 2\pi \frac{R}{\lambda}[\sin(\phi_m) - \sin(\phi_n)] \quad (5)$$

where ϕ_m is the angle of *m*-th antenna in azimuthal planes, then:

$$\sin(\alpha) = \frac{K1}{\sqrt{K1^2+K2^2}}, \quad \cos(\alpha) = \frac{K2}{\sqrt{K1^2+K2^2}}, \quad Z_c = \sqrt{K1^2+K2^2} \quad (6)$$

The mathematical expressions for real and imaginary components of spatial correlation between *m*-th and *n*-th antenna at the receiver for the case of ULA antenna are given as [10]:

$$\mathrm{Re}\{Rr(m,n)\} = J_0(Z_c) + 2\sum_{k=1}^{\infty} \frac{a^2(1-e^{-a\pi})}{a^2+4k^2} J_{2k}(Z_c)\cos(2k\theta) \quad (7)$$

$$\mathrm{Im}\{Rr(m,n)\} = 4C_l \sum_{k=0}^{\infty} \frac{a^2(1+e^{-a\pi})}{a^2+(2k+1)^2} \cdot J_{2k+1}(Z_l)\sin[(2k+1)\theta] \quad (8)$$

where $Z_l = 2\pi(m-n)d/\lambda$ and *d* is antenna spacing.

The above expressions (1) (2) and (7) (8) can be applied to determine spatial correlations between any two antenna elements in UCA or ULA receiving antennas. Note that these expressions do not include the effect of antenna mutual coupling. This condition is approximately fulfilled when the antenna element spacing is about half of the wavelength or more.

Figure 2 shows the spatial correlation between two antenna elements (1 and 2) of a UCA or ULA antenna when the central AOA is 30°, 60° and 90°. There are three curves in each plot. These curves correspond to a different decay factor *a* of 3, 10 and 30.

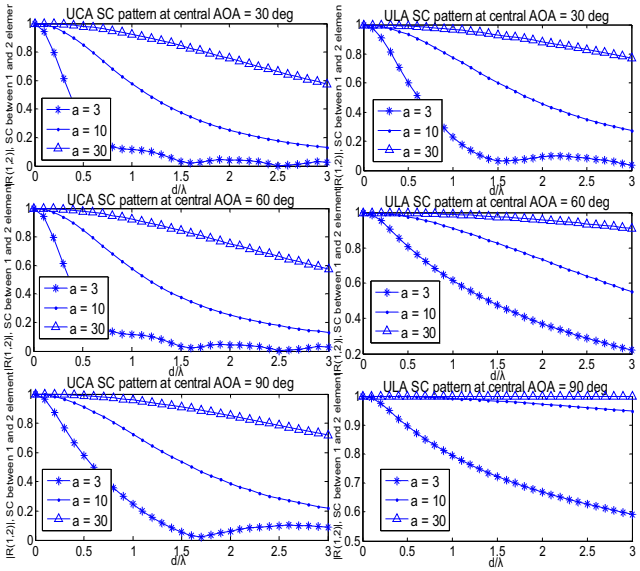

Fig. 2 Spatial correlation between antenna 1 and 2 for UCA *and* ULA at AOA of 30°, 60° and 90°

From the results presented in Figure 2, it is apparent that for the same antenna spacing d/λ the spatial correlation in ULA is higher than that in UCA when the central AOA increases from 30° to 90°. This can be due to the fact that ULA offers limited diversity when signals arrive from directions close to the ULA end-fire direction. UCA eliminates this deficiency as it offers almost a uniform view angle for all directions.

B. Channel model

A flat block-fading narrow-band MIMO system with M_t array antennas at transmitter and M_r array antennas at receiver is considered. The relationship between the received and transmitted signals is given by (9):

$$Y_s = HS + V \tag{9}$$

where Y_s is the M_r x N complex matrix representing the received signals; S is the M_t x N complex matrix representing transmitted signals; H is the M_r x M_t complex channel matrix and V is the M_r x N complex zero-mean white noise matrix. N is the length of transmitted signal. The channel matrix H describes the channel properties which depend on antenna array configuration and signal propagation environment.

In order to simulate properties of the MIMO channel we apply the Kronecker model [11] [12]. In this model, the transmitter and receiver correlations are assumed to be separable and the channel matrix H is represented as:

$$H = R_R^{1/2} H_g R_T^{1/2} \tag{10}$$

where H_g is a matrix with identical independent distributed (i.i.d) Gaussian entries with zero mean and unit variance and R_R and R_T are spatial correlation matrices at the receiver and transmitter, respectively. Note that the assumption of i.i.d. requires a scattering-rich signal propagation environment. For the array configurations shown in Figure 1, the correlation experienced by pairs of transmitting antennas can be written as [13]:

$$R_t(m,n) = J_0[2\pi(m-n)/\lambda] \tag{11}$$

Therefore, the correlation matrix R_t for the MS transmitting antennas can be generated using (12)

$$R_t = \begin{bmatrix} R_t(1,1) & \cdots & R_t(1,M_t) \\ \vdots & \ddots & \vdots \\ R_t(M_t,1) & \cdots & R_t(M_t,M_t) \end{bmatrix} \tag{12}$$

In turn, the correlation matrix for the receiving antennas, R_r, can be obtained using equations (1) (2) and (7) (8) and can be shown to be given as (13).

$$R_r = \begin{bmatrix} R_r(1,1) & \cdots & R_r(1,M_r) \\ \vdots & \ddots & \vdots \\ R_r(M_r,1) & \cdots & R_r(M_r,M_r) \end{bmatrix} \tag{13}$$

Having determined R_t and R_r, the channel matrix H can be calculated using equation (10).

III. MIMO Channel Capacity with Perfect Knowledge of Channel Matrix

A. MIMO Channel Capacity & EDOF

If CSI is perfectly known at the receiver but unknown at the transmitter, the capacity of a MIMO system with M_r receive antennas and M_t transmit antennas can be determined using [3][4]:

$$C = E(\log_2\{\det[I_{M_R} + \frac{\rho}{M_t}(HH^H)]\}) \tag{15}$$

where $\{.\}^H$ stands for the transpose-conjugate; ρ is the total transmitted SNR.

An alternative expression for the capacity in such a case can be obtained by decomposing the channel into $n = min(M_r, M_t)$ virtual single input single output (SISO) sub-channels, and can be shown to be given as (16),

$$C = \sum_i^n \log_2(1 + \frac{\rho_i}{n}\lambda_i) \tag{16}$$

where $\rho = \sum_i^n \rho_i$ and the gains of sub-channels are represented by the eigenvalues of the channel correlation matrix HH^H.

Here, it is assumed that the transmitted power is equally allocated to each sub-channel, which is easy to accomplish in practice. The channel capacity can be further maximized by applying power allocation schemes such as 'water-filling'. However, this scheme requires a feedback to pass CSI from the receiver to the transmitter, which is not easy in practice.

It has to be noted that the MIMO channel capacity can be related to the channel effective degree of freedom (EDOF) [14]. In order to determine EDOF, the channel matrix properties and the signal to noise ratio (SNR) are required. According to [14], the EDOF is defined as:

$$EDOF \equiv \frac{d}{d\delta} C(2^{\delta}\rho)\Big|_{\delta=0} \quad (17)$$

Given the eigenvalues of the channel correlation HH^{H}, it can be rewritten as

$$\frac{d}{d\delta} C(2^{\delta}\rho)\Big|_{\delta=0} = \frac{d}{d\delta}\sum_{i}^{n}[\log_2(1+\frac{2^{\delta}\rho}{n}\lambda_i)]\Big|_{\delta=0} = \sum_{i}^{n}\frac{\frac{\rho}{n}\lambda_i}{1+\frac{\rho}{n}\lambda_i} \quad (18)$$

It is apparent that when $\rho\lambda_i/n >> 1$, (18) is approximately equal to n and EDOF becomes maximum. In this case, every sub-channel is useful to transmit signals. In turn, when $\rho\lambda_i/n < 1$, EDOF is smaller than n, some sub-channels are not efficient to transmit signals. Reasons for the reduced EDOF can be due to an increased level of channel correlation and decreased SNR.

B. Numerical Results

Based on the presented theory, the channel EDOF and capacity are simulated assuming that a ULA is present at the transmitter and either a UCA or ULA is located at the receiver. Simulations are performed for different values of the central AOA, decay factor, SNR and varying numbers of transmit/receive antennas.

The first investigated scenario is when 4-element array antennas are used at the transmitter and receiver of a MIMO system. The spacing d between adjacent elements of ULA or the radius R of UCA at transmitter is set at 0.5 wavelength (λ). To reduce the antenna mutual coupling (which is neglected here) and correlation, d and R can be made larger than 0.5λ. Figures 3, 4, 5 and 6 show EDOF and capacity as a function of SNR for both UCA and ULA for three values of decay factor a, and for the central AOA equal to 0°, 30°, 60° and 90°.

The presented results reveal that both EDOF and capacity increase when SNR increases. At a higher decay factor, both EDOF and capacity are lower. This can be explained by the fact that a larger decay factor corresponds to a smaller angle spread (AS) indicating a higher spatial correlation level. EDOF and capacity are degraded due to correlation.

In Figure 3 and 4, one can see that for the central AOA of 0° and 30° both EDOF and capacity for ULA are higher than for UCA for the three chosen values of decay factor.

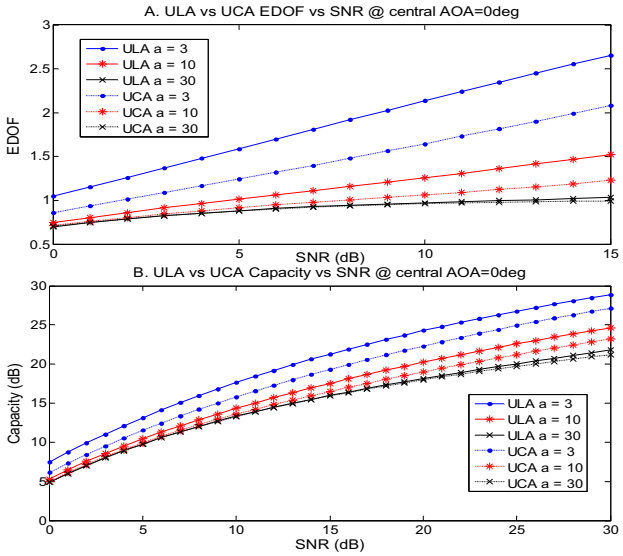

Fig. 3 EDOF and Capacity of UCA and ULA vs SNR at central AOA=0 ° for two values of decay factor a of 3 and 10.

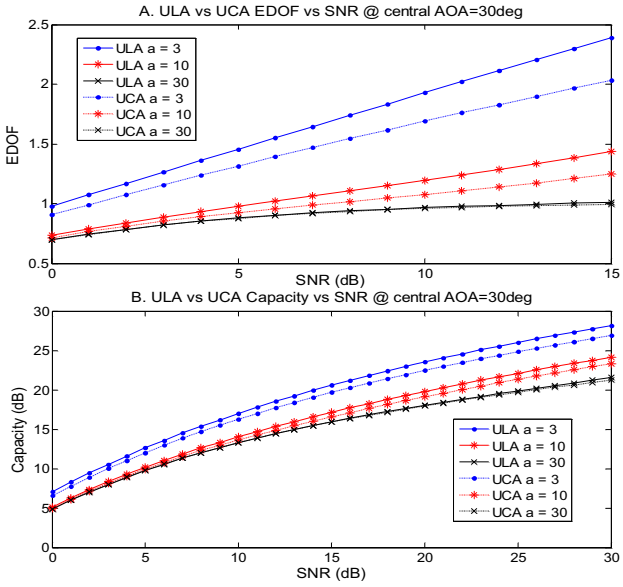

Fig. 4 EDOF and Capacity of UCA and ULA vs SNR at central AOA=30 ° for two values of decay factor a of 3 and 10.

However, when the central AOA is increased to 60° and 90° an opposite result is observed in Figure 5 and 6. In the latter case, performance of UCA is superior in comparison with ULA. These opposite trends indicate that at a certain value of central AOA, the performances of UCA and ULA should be equal.

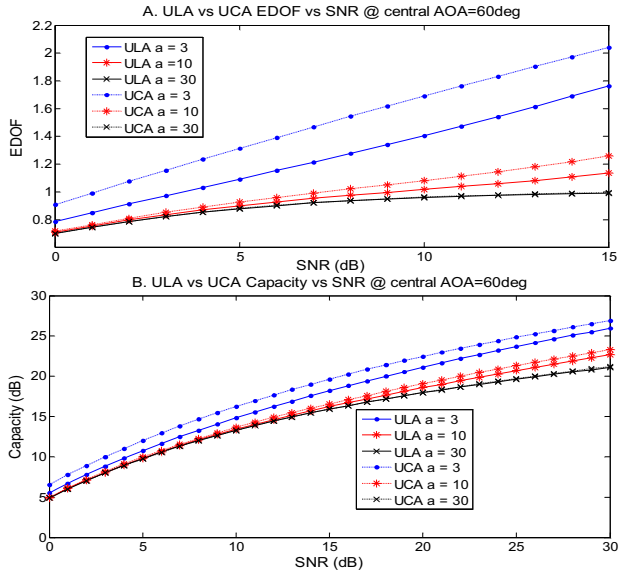

Fig. 5 EDOF and Capacity of UCA and ULA vs SNR at central AOA=60° for two values of decay factor a of 3 and 10.

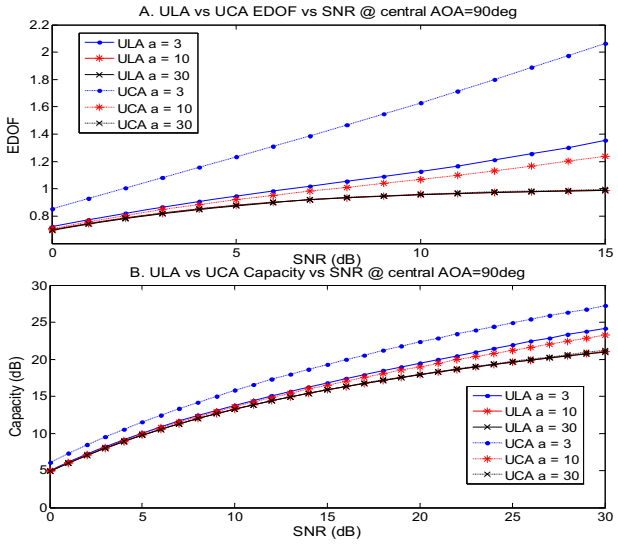

Fig. 6 EDOF and Capacity of UCA and ULA vs SNR at central AOA=90°for two values of decay factor a of 3 and 10.

In order to determine the cross point (for EDOF or capacity) further simulations are performed. The results are shown in Figure 7. One can see in Figure 7 that both EDOF and capacity decrease for the case of ULA when the central AOA increases at two different SNR. This is because the ULA's spatial correlation level increases as the central AOA gets larger. This degrades channel capacity. The cross point is between AOA=40° and AOA=50°. To the left of the cross point, EDOF and capacity of ULA is higher than for UCA. In turn, on the right hand side, UCA's performance is better.

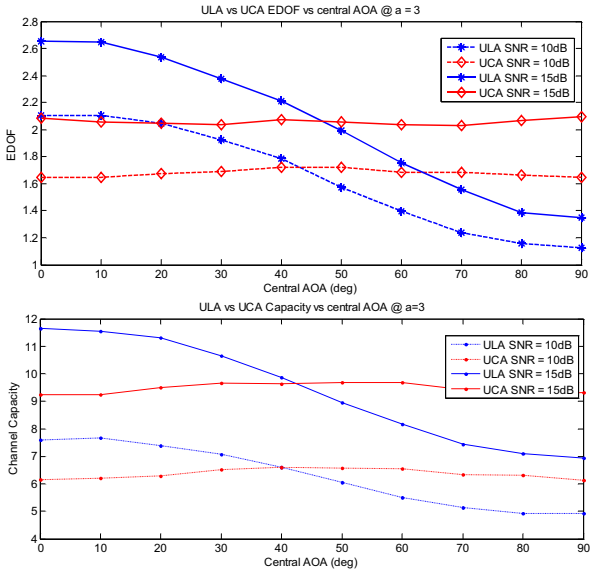

Fig. 7 EDOF and Capacity of UCA and ULA vs central AOA

Using the earlier described settings for the 4x4 MIMO, the number of receiving antenna elements is increased and then the spatial correlation patterns and channel capacity versus the number of transmit and receive antennas are simulated.

Because of a usually small size of the mobile station, the number of transmitting antennas is limited. This is not the case of base station which offers a larger available area where more antennas can be added. Here, the number of antenna elements in a ULA is assumed to increase along the line with same spacing d, as shown in Figure 8A. In turn, for a UCA the number of antenna elements with the same spacing d increases on the circle, as shown in Figure 8B. In the UCA case, when the number of elements on the circle increases with spacing d unchanged, the radius R increases correspondingly.

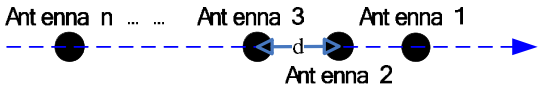

A. ULA

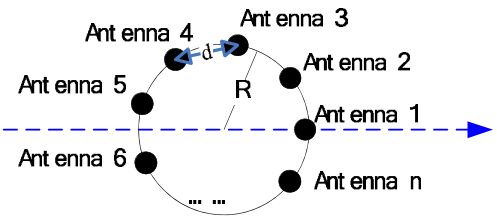

B. UCA

Fig. 8 ULA and UCA antenna arrays

Figure 9 presents the spatial correlation between antenna elements 1 and 2 for receiving UCA and ULA for the new settings. From Figure 9A, one can see that when the number of antenna elements increases the spatial correlation for UCA varies from 0 to 1. However, the variation due to an increased

number of antenna elements is very small. For the ULA case, the spatial correlation level of receiving antennas is unchanged when the number of antennas increases.

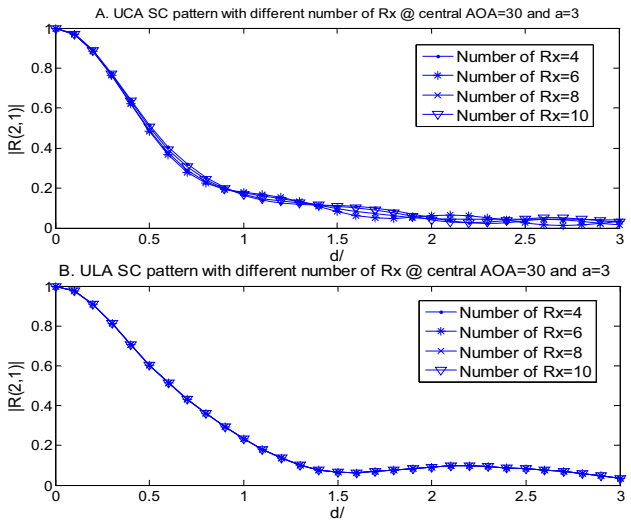

Fig. 9 Spatial correlation between antenna 1 and antenna for different numbers (4,6,8, and 10) of antenna elements in receiving UCA (A) and ULA (B) antenna arrays at central AOA of 30° and decay factor a of 3.

Similarly as Figure 3-6, Figures 10, 11 and 12 show the results for channel capacity for a different number of receiving antenna elements for the cases of ULA and UCA receiving antennas. An increase in the number of antenna elements in ULA and UCA brings improvement to the channel capacity. The cross points between red curves representing ULA and blue curves standing for UCA move to the right as the number of antennas increases. When the number of receiving antenna elements is 10, the capacity of ULA is superior to UCA for the central AOA of 0^o to 50^o.

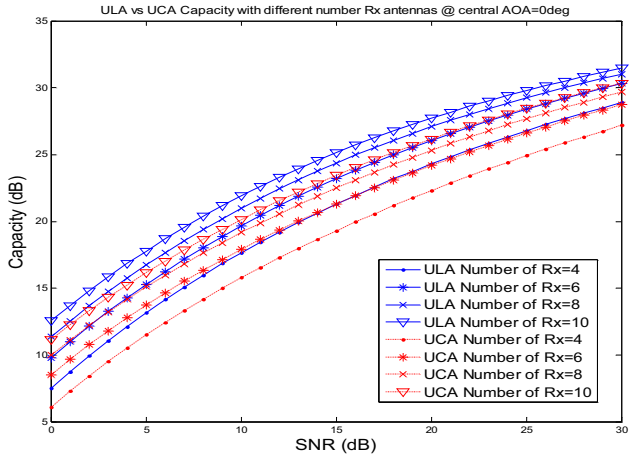

Fig. 10 ULA vs UCA capacity with different number of Rx antenna array elements at decay factor a equal to 3 and central AOA equal to 0^o

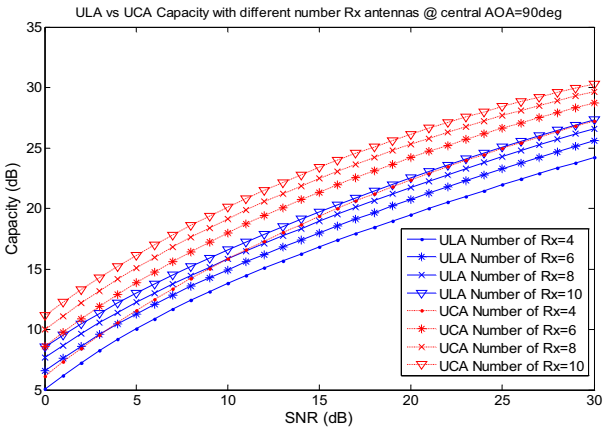

Fig. 11 ULA (blue lines) vs UCA (red lines) capacity for different number of Rx antenna array elements at decay factor a equal to 3 and central AOA equal to 90^o

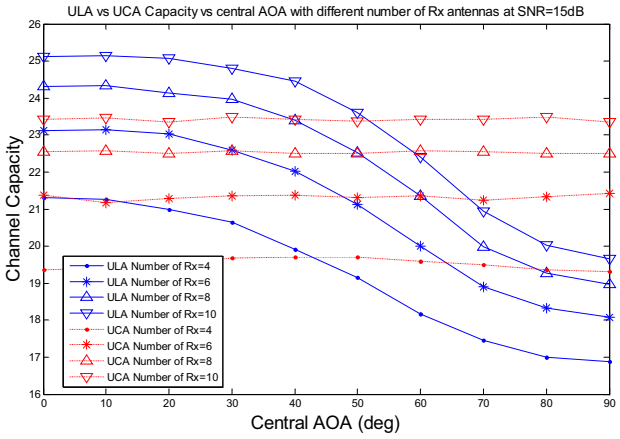

Fig. 12 ULA vs UCA capacity with different number of Rx antenna array elements decay factor a equal to 3

IV. MIMO Channel Capacity with Channel Estimation Errors

A. *Training –based Channel Estimation*

For the training based channel estimation method, the relationship between the received signals and the training sequences is given by equation (19) as

$$Y = HP + V \tag{19}$$

Here the transmitted signal S in (1) is replaced by P, which represents the M_t x L complex training matrix (sequence) where L is the length of the training sequence. The goal is to estimate the complex channel matrix H from the knowledge of Y and P. The transmitted power in the training mode is assumed to be given by a constant value. According to [7] and [8], the estimation using SLS or MMSE method requires orthogonality of the training matrix P. In the undertaken analysis, the training matrix P is assumed to satisfy this condition.

The performance of SLS method can be obtained by scaling up the results from the least square (LS) method. Using the LS method, the estimated channel can be written as [15],

$$\hat{H}_{LS} = YP^{\dagger} \tag{20}$$

where $\{.\}^{\dagger}$ stands for pseudo-inverse. The mean square error (MSE) of the LS method is given as

$$MSE_{LS} = E\{\left\| H - \hat{H}_{LS} \right\|_F^2\} \tag{21}$$

in which $E\{.\}$ denotes a statistical expectation. According to [7] and [8], the minimum value of MSE for the LS method is given as

$$MSE_{\min}^{LS} = \frac{M_t^2 M_r}{\rho_t} \tag{22}$$

in which ρ^t stands for transmitted SNR in training mode.

The SLS method reduces the estimation error of the LS method and the improvement is given by the scaling factor γ as

$$\gamma = \frac{tr\{R_H\}}{MSE_{LS} + tr\{R_H\}} \tag{23}$$

The estimated channel matrix is represented by [7], [8]

$$\hat{H}_{SLS} = \frac{tr\{R_H\}}{\sigma_n^2 M_r + tr\{(PP^H)^{-1}\} + tr\{R_H\}} YP^{\dagger} \tag{24}$$

Here, σ_n^2 is the noise power; R_H is the channel correlation matrix defined as $R_H=E\{H^H H\}$ and $tr\{.\}$ implies the trace operation.

The MSE for SLS is given as [7] [8]

$$\begin{aligned} MSE_{SLS} &= E\{\left\| H - \gamma \hat{H}_{LS} \right\|_F^2\} \\ &= (1-\gamma)^2 tr\{R_H\} + \gamma^2 MSE_{LS} \end{aligned} \tag{25}$$

The minimized MSE of MMSE method can be written as [7] [8]

$$MSE_{\min}^{SLS} = \frac{MSE_{LS} tr\{R_H\}}{MSE_{LS} + tr\{R_H\}} \tag{26}$$

By taking into account expression (23), the minimized MSE of the SLS method (27) can be rewritten as

$$\begin{aligned} MSE_{SLS} &= [(tr\{R_H\})^{-1} + \frac{\rho_t}{M_t^2 M_r}]^{-1} \\ &= [(\sum_i^n \lambda_i)^{-1} + \frac{\rho_t}{M_t^2 M_r}]^{-1} \end{aligned} \tag{27}$$

where $n=min(M_r, M_t)$ and is λ_i the i-th eigenvalue of the channel correlation R_H.

In the MMSE method, the estimated channel matrix is given as (28) [7] [8],

$$\hat{H}_{MMSE} = Y(P^H R_H P + \sigma_n^2 M_r I)^{-1} P^H R_H \tag{28}$$

The MSE of MMSE estimation is given as

$$MSE_{MMSE} = E\{\left\| H - \hat{H}_{MMSE} \right\|_F^2\} = tr\{R_E\} \tag{29}$$

in which R_E is estimation error correlation written as

$$\begin{aligned} R_E &= E\{(H - \hat{H}_{MMSE})(H - \hat{H}_{MMSE})^H\} \\ &= (R_H^{-1} + \sigma_n^{-2} M_r^{-1} PP^H)^{-1} \end{aligned} \tag{30}$$

The minimized MSE for MMSE is obtained as [7][8]

$$MSE_{MMSE} = tr\{(\Lambda^{-1} + \sigma_n^{-2} M_r^{-1} Q^H PP^H Q)^{-1}\} \tag{31}$$

In (32), Q is the unitary eigenvector matrix of R_H and Λ is the diagonal matrix with eigenvalues of R_H. The minimized MSE for the MMSE method, given by equation (31), can be rewritten using the orthogonality properties of the training sequence P and the unitary matrix Q, as shown by

$$\begin{aligned} MSE_{MMSE} &= tr\{(\Lambda^{-1} + \rho_t M_r^{-1} I)^{-1}\} \\ &= \sum_i^n (\lambda_i^{-1} + \rho_t M_r^{-1})^{-1} \end{aligned} \tag{32}$$

From equation (27), (31) and (32), one can see that MSE of SLS and MMSE methods depends on the channel correlation which, in turn, is affected by the transmitter and receiver spatial correlations.

B. Channel Capacity Taking Into Account Channel Estimation Errors

In practice, MIMO channel capacity is governed by two factors. One is EDOF and the other one is the availability of CSI at the receiver. In equation (16), the channel matrix H is assumed to be perfectly known at the receiver. This is an ideal case. In practice, H has to be replaced by an estimated channel matrix, which carries estimation errors. For the training-based channel estimation methods like SLS and MMSE, the estimation error is affected by the number of antenna array elements and the spatial correlation. Increasing the number of antenna array elements can improve the channel capacity, as shown by expressions (16) or (17). However, when larger size antennas are used estimating the channel can be a more difficult tusk. Here, we further investigate the effect of channel estimation on the capacity of MIMO system, which has been addressed in [16] [17] and [18].

Assuming that the channel estimation error is denoted by e, the estimated channel matrix $\hat{H}$ can be written as

$$\hat{H} = H + e \tag{33}$$

The received signal can accordingly be written as,

$$Y = \hat{H}S + eS + V \tag{34}$$

Correlation of e can be expressed as

$$R_E = E\{(H - \hat{H})(H - \hat{H})^H\} = \sigma_e^2 I \tag{35}$$

in which σ_e^2 is the error variance. (In [16] and [17], the error variance is defined in a slightly different way.) Using equation (21), we have

$$\sigma_e^2 = \frac{MSE}{M_r} \tag{36}$$

The channel capacity of MIMO system with an imperfectly known H at the receiver is defined as the maximum mutual information between Y and S and is given by

$$C = \max_{tr\{Q\}\le P} \{I(S;Y,\hat{H})\} \tag{37}$$

If the transmitter does not have any knowledge of the estimated channel, the mutual information in equation (37) can be written as [16] [17] [18] [19],

$$I(S;Y,\hat{H}) = I(S;Y \mid \hat{H}) = h(S \mid \hat{H}) - h(S \mid Y,\hat{H}) \tag{38}$$

Because adding any term dependent on Y does not change the entropy [17], then

$$h(S \mid Y,\hat{H}) = h(S - uY \mid Y,\hat{H}) \tag{39}$$

in which u is the MMSE estimator given by

$$u = \frac{E\{SY^H \mid \hat{H}\}}{E\{YY^H \mid \hat{H}\}} \tag{40}$$

Combining the above expression with expression (35), the following is obtained

$$\begin{aligned} u &= \frac{E\{S(\hat{H}S + eS + V)^H \mid \hat{H}\}}{E\{(\hat{H}S + eS + V)(\hat{H}S + eS + V)^H \mid \hat{H}\}} \\ &= \frac{Q\hat{H}^H}{\hat{H}Q\hat{H}^H + E\{eQe^H\} + \sigma_n^2 I_{M_r}} \end{aligned} \tag{41}$$

where $Q=E\{SS^H\}$ is a M_t by M_t autocorrelation matrix of transmitted signal S.

The autocorrelation matrix holds the property that the *trace(Q)* is equal to the total transmitted signal power P_s , which is used in evaluating $\rho=P_s/\sigma_n^2$. If we assume the special case of M_t equal to M_r and that the transmitted signal power is equally allocated to transmitting antennas, (41) can be rewritten as

$$\begin{aligned} u &= \frac{Q\hat{H}^H}{\hat{H}Q\hat{H}^H + Q\sigma_e^2 I_{M_r} + \sigma_n^2 I_{M_r}} \\ &= \frac{p\hat{H}^H}{p\hat{H}\hat{H}^H + p\sigma_e^2 I_{M_r} + \sigma_n^2 I_{M_r}} \end{aligned} \tag{42}$$

in which $p=P_s/M_t$ is the power allocated to each transmitting antenna.

Using

$$h(S - uY \mid \hat{H}) = h(S - uY \mid Y,\hat{H}) \tag{43}$$

and the fact that hat conditioning decreases the entropy,

$$I(S;Y \mid \hat{H}) = h(S \mid \hat{H}) - h(S - uY \mid Y,\hat{H}) \tag{44}$$

For the case of $S \mid \hat{H}$ and $(S - uY \mid Y,\hat{H})$ having a Gaussian distribution, (44) can be expressed as [16] [17] [18],

$$\begin{aligned} I(S;Y \mid \hat{H}) \ge\ & E\{\log_2[\det(\pi eQ)]\} - \\ & E\{\log_2[\det(\pi eE\{(S-uY)(S-uY)^H \mid \hat{H}\})]\} \\ \ge\ & E\{\log_2[\det(I_{M_r} + \frac{p\hat{H}\hat{H}^H}{I_{M_r}(p\sigma_e^2 + \sigma_n^2)})]\} \end{aligned} \tag{45}$$

The lower bound of the ergodic channel capacity can be shown to be given as

$$\begin{aligned} C &= E\{\log_2[\det(I_{M_r} + \frac{p\hat{H}\hat{H}^H}{p\sigma_e^2 + \sigma_n^2})]\} \\ &= E\{\log_2[\det(I_{M_r} + \frac{\frac{P_s}{M_t}\hat{H}\hat{H}^H}{\sigma_n^2}\frac{1}{1+\frac{P_s}{M_t}\frac{\sigma_e^2}{\sigma_n^2}})]\} \\ &= E\{\log_2[\det(I_{M_r} + \frac{\rho_{SNR}\hat{H}\hat{H}^H}{M_t}\frac{1}{1+\frac{\rho_{SNR}}{M_t}\frac{MSE}{M_r}})]\} \end{aligned} \tag{46}$$

Equation (46) indicates that the MIMO system capacity is a function of SNR, the estimated channel matrix $\hat{H}$ and the channel estimation error σ_e^2. This expression shows that the channel properties and the quality of channel estimation influence the capacity. The influence of channel estimation errors on capacity will be investigated in the next section.

C. Numerical Results

In the first instance, the SLS and MMSE channel estimation methods are assessed via computer simulations. In the undertaken simulations, the transmitter of the MIMO system is assumed to be equipped with ULA while the receiver uses either UCA or ULA. The case of 4x4 MIMO system is considered. The simulations are performed for different values of central AOA, decay factor *a* and the transmitted SNR ($\rho_t = \rho$). The other assumptions are similar to the ones already described in section 3.2.

Simulations of MSE as a function of ρ ($\rho=P_s/\sigma_n^2$) for the SLS and MMSE channel estimation are performed for two decay factors of 3 and 30 assuming the central AOA of 0^o, 30^o, 60^o and 90^o. The results are shown in Figure 13, 14, 15 and 16.

In all of the cases presented in Figure 13, 14, 15 and 16 it is apparent that when ρ increases MSE decreases for both SLS and MMSE irrespectively from the choice of decay factor. MSE of SLS looks to be independent of the decay factor. Also only negligible changes in MSE of SLS are observed when CLA

replaces ULA at the receiver. However, MSE of MMSE is sensitive to the choice of decay factor and is smaller for larger decay factors.

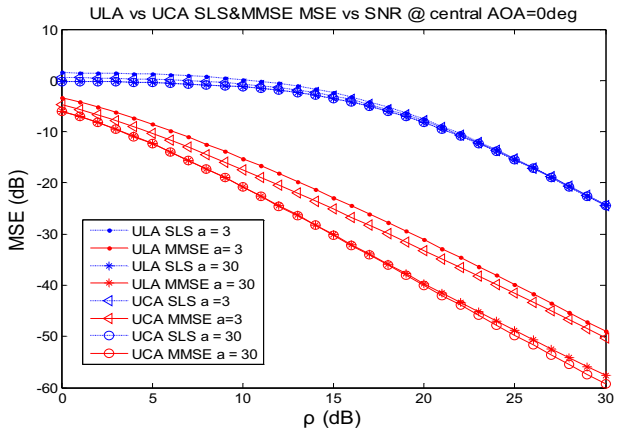

Fig. 13 MSE vs ρ for receiving ULA (blue lines) and UCA (red lines) at central AOA=0°

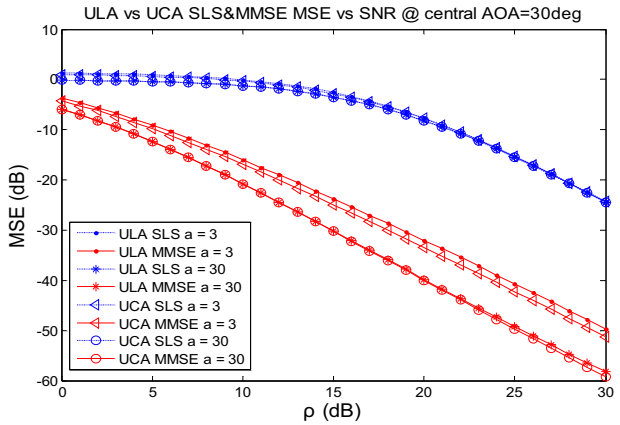

Fig. 14 MSE vs ρ for UCA and ULA at central AOA=30°

With reference to the choice of the central AOA of 0° and 30° in Figure 13 and 14, one can see that MSE of MMSE for ULA is larger than for UCA.

This happens irrespectively of the choice of the decay factor value. However, in the case of central AOA of 60° and 90°, shown in Figure 15 and 16, one can see that the opposite conclusion takes place. The MSE of MMSE for the UCA is getting greater than when the ULA is used at the receiver.

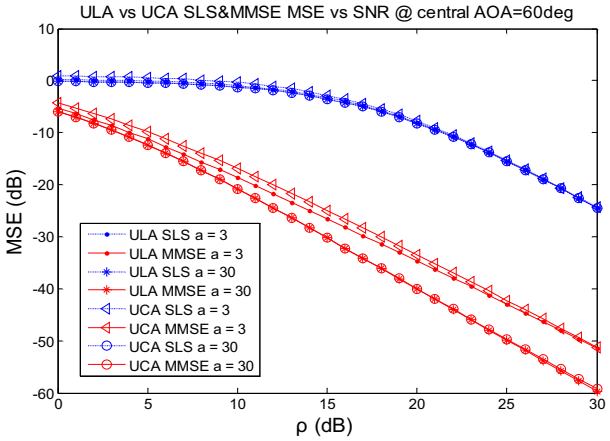

Fig. 15 MSE vs ρ for receiving ULA (blue lines) and UCA (red lines) at central AOA=60°

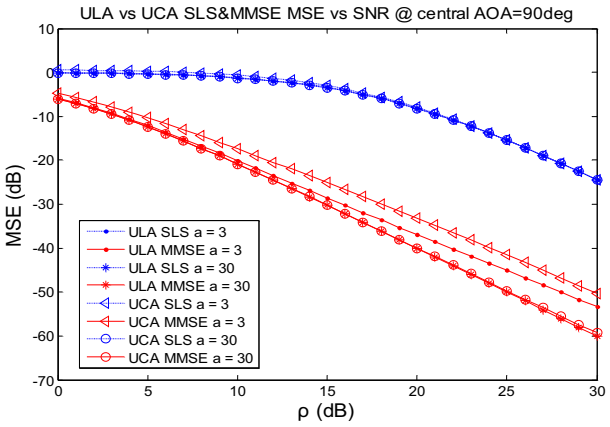

Fig. 16 MSE vs ρ for receiving ULA (blue lines) and UCA (red lines) at central AOA=90°

Figure 17 shows the simulated results for MSE versus central AOA for two cases of ρ equal to 15dB and 20dB, respectively. One can see that when ρ is equal to 15dB, MSE of MMSE for ULA is larger than for UCA when the central AOA is smaller than 50°. In turn, when the central AOA is larger than 50° an opposite situation takes place: MSE of MMSE for UCA is larger than the one for ULA.

Similar observations are made when ρ is equal to 20dB. However, in this case the central AOA cross point is moved to about 60°.

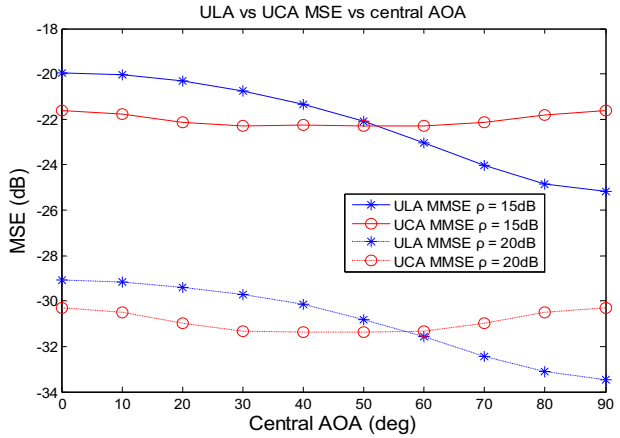

Fig. 17 MSE vs central AOA for ULA (blue line) and UCA (red line) at decay factor a equal to 3

Figure 18 show the results for MSE similar to those of Figure 17. However, they are obtained for different number of receiving antenna elements of 4, 6, 8 and 10.

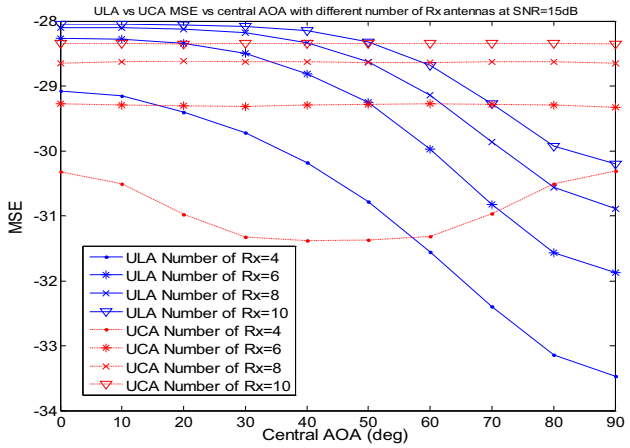

Fig. 18 MSE vs central AOA for different number of antenna elements in receiving ULA (blue lines) and UCA (red lines) at decay factor a equal to 3 and ρ equal to 20dB

It can be seen in Figure 18 that when the receiving array includes 4 antenna elements, the channel estimation shows the best performance for both ULA and UCA. When the number of antenna elements is increased from 4 to 6, 8 and 10, the channel estimation accuracy is getting worse for both ULA and UCA cases. These results confirm our expectation that larger size MIMO systems face the problem of decreased estimation of MIMO channel.

In the next step, we carry out investigations how the channel estimation errors affect MIMO capacity. In simulations, we apply equation (48). The cases of ULA and UCA at the receiver are considered.

Figure 19 presents the MIMO capacity versus central AOA with and without channel estimation errors.

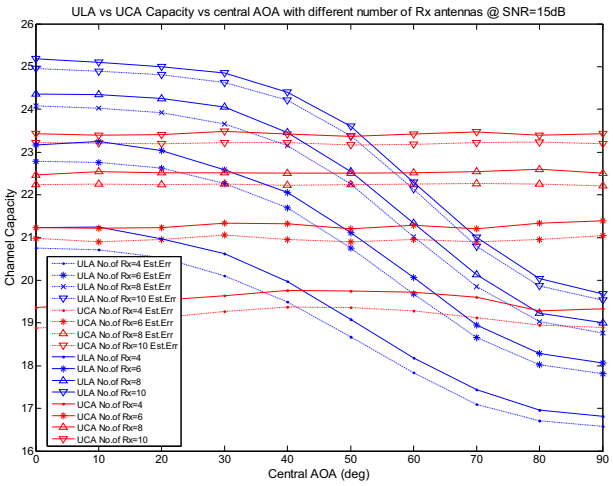

Fig. 19 Channel capacity without (continuous lines) and with (broken lines) channel estimation error vs central AOA for different numbers (4,6, 8 and 10) of antenna elements in receiving ULA (blue lines) and UCA (red line) at decay factor a equal to 3 and ρ equal to 20dB.

One can see from Figure 19 that the determined MIMO capacities taking into account the channel estimation errors are always lower than the ones calculated using the assumption that the ideal channel state information is available to the receiver. However, for the assumed conditions the differences are not highly pronounced. The two sets of curves (without and with estimation errors) are similar in shape and are displaced in the vertical direction by a small value.

V. Conclusion

In this paper, we have reported on investigations into channel estimation and channel capacity of a MIMO system employing Uniform Linear Array at the transmitter and either a Uniform Circular Array or Uniform Linear Array at the receiver. In the presented investigations, the transmitter is assumed to be surrounded by scattering objects while the receiver is postulated to be free of scatterers. The signal angle of arrival (AOA) has been assumed to follow the Laplacian distribution. The angle spread (AS) is characterized by the decay factor.

The attention has been paid to the effect of different spatial correlation in receiving linear and circular arrays. The obtained results have shown that for the central AOA varying from 0^o to 90^o, UCA's spatial correlation pattern (as a function of element antenna spacing) is relatively constant while ULA's spatial correlation level increases; both UCA's and ULA's spatial correlation patterns are not sensitive to the increased number of array elements. At a larger decay factor corresponding to a smaller angular spread (and thus a higher level of spatial correlation), the MSE of training based channel estimation methods such as SLS and MMSE is reduced for both the UCA and ULA receiving antenna cases. This agrees with the findings of [2] and [20]. Other presented results have concerned the variation of MSE as a function of central AOA varying from 0^o to 90^o when the signal to noise ratio ρ is equal to 15dB or 20dB. It has been shown that at ρ=15dB, MSE of MMSE for ULA is higher in comparison with UCA when the central AOA is

smaller than 50^o. When central AOA becomes larger than 50^o, the UCA performance is better in terms of lower value of MSE. For ρ of 20dB a similar trend has been observed but the cross point occurs for the central AOA equal to 60^o. When the number of receiving antennas increases, the performance gets worse in terms of MSE for both ULA and UCA cases.

The obtained results have also shown that for a larger decay factor, the channel capacity is reduced for both UCA and ULA receiving antennas. The 4x4 MIMO system employing the receiving ULA shows higher capacity when the central AOA is smaller than 40^o. For central AOA greater than 50° the opposite happens and the system using UCA outperforms the one using ULA. When the number of receiving antennas increases, improvements to channel capacity are demonstrated for both ULA and UCA. The cross points for ULA and UCA capacity curves move to the right when the number of antennas increases. When the number of receiving antennas is 10, the capacity performance for ULA is superior to UCA for central AOA of 0^o to 50^o.

The channel capacity determined by including the channel estimation errors is lower in comparison with the capacity calculated assuming perfect knowledge of channel matrix. This result is irrespective of the fact whether ULA or UCA antennas are used at the MIMO receiver.

REFERENCES

[1] J. Tsai, R. M. Buehrer and B. D. Woerner, "BER performance of a uniform circular arrays versus a uniform linear array in a mobile radio environment", IEEE Trans. on wireless comms., Vol. 3, No. 3, pp. 695-700, May 2004

[2] X. Liu, S. Lu, M. E. Bialkowski and H.T. Hui, "MMSE Channel estimation for MIMO system with receiver equipped with a circular array antenna", Proc. 2007 Asia Pacific Microwave Conference, APMC2007, pps. 1-4, Dec. 2007

[3] E. Telatar, "Capacity of multi-antenna Gaussian channels," Eur. Trans. Telecommun, vol. 10, no. 6, pp. 585-596, Nov. 1999

[4] T. L. Marzetta and B. M. Hochwald, "Capacity of a mobile multiple-antenna communication link in Rayleigh flat fading," IEEE Trans. Information Theory, vol. 45, no. 1, pp. 139-157, Jan. 1999

[5] A. Narula, M. J. Lopez, M. D. Trott, and G. W. Wornell, "Efficient use of side information in multiple-antenna data transmission over fading channels," IEEE J. Select. Areas Commun., vol. 16, no. 8, pp. 1423-1436, Oct. 1998

[6] C. Budianu and L. Tong, "Channel estimation for space-time orthogonal block codes", IEEE Trans. Signal Process., Vol. 50, pp. 2515-2528, Oct, 2002

[7] M. Biguesh and A. B. Gershman, "MIMO channel estimation: optimal training and tradeoffs between estimation techniques," Proc. ICC'04, Paris, France, June 2004

[8] M. Biguesh and A. B. Gershman, "Training-based MIMO channel estimation: a study of estimator tradeoffs and optimal training signals," IEEE Trans. Signal Processing, Vol. 54, No. 3, Mar. 2006

[9] J. Tsai, R. M. Buehrer and B. D. Woerner, "Spatial fading correlation function of circular antenna arrays with Laplacian Energy distribution," IEEE Comms. Letters, Vol. 6, No. 5, pps.178-180, May 2002

[10] J. Tsai, R. M. Buehrer and B. D. Woerner, "The impact of AOA energy distribution on the spatial fading correlation of linear antenna array", Vol. 2, pp. 933-937, IEEE 5th VTC, May 2002

[11] E. G. Larsson and P. Stoica, "Space-time block coding for wireless communication", Cambridge University Press, 2003

[12] C. N. Chuah, D. N. C. Tse, and J. M. Kahn, "Capacity scaling in MIMO wireless systems under correlated fading," IEEE Trans. Information Theory, vol. 48, pp. 637-650, Mar. 2002

[13] W. C. Jakes, Microwave Mobile Communications, New York: John Wiley & Sons, 1974

[14] D, Shiu, J. Foschini, M. J. Gans and J. M. Kahn, "Fading correlation and its effect on the capacity of multielemnt antenna system," IEEE Trans. on Commun., vol 48, no. 3, Mar. 2000

[15] S. M. Kay, "Fundamentals of Statistic Signal Processing: Estimation Theory", Prentice-Hall, Inc., 1993

[16] T. Yoo, A. Goldsmith, "Capacity and power allocation for fading MIMO channels with channel estimation error", IEEE Trans. Information Theory, vol. 52, No.5, May 2006

[17] T. Yoo, A. Goldsmith, "Capacity of fading MIMO channels with channel estimation error", IEEE Int. Conf. on Communications, vol. 2, pp. 808-813, Jun. 2004

[18] M. Torabi, M. R. Soleymani and S. Aissa, "On the performance of MIMO-OFDM systems with imperfect channel information," Int. Conf. on wireless networks, communications and mobile computing, vol. 1, pp. 600-605, June 2005

[19] M. Medard, "The effect upon channel capacity in wireless communications of perfect and imperfect knowledge of the channel," IEEE Trans. Information Theory, vol. 46, pp. 933-946, May 2000

[20] X. Liu, M. E. Bialkowski and S. Lu, "Investigations into Training-Based MIMO Channel Estimation for Spatial Correlated Channels", Proc IEEE AP-S Symposium, Hawaii, USA, 2007

X. Liu received his Bachelor degree in Communication Engineering from Zhejiang University of Technology (ZJUT), China in June 2005. In July 2006, he obtained his Master degree in Telecommunication Engineering from the University of Queensland, Australia. Now he is a PhD candidate in the School of Information Technology and Electrical Engineering at the University of Queensland researching channel estimation methods for Multiple Input Multiple Output (MIMO) wireless communication systems. He is a holder of the University of Queensland Research Scholarship (UQRS).

M. E. Bialkowski received the M.Eng.Sc. degree (1974) in applied mathematics and the Ph.D. degree (1979) in electrical engineering both from the Warsaw University of Technology and a higher doctorate (D.Sc. Eng.) in computer science and electrical engineering from the University of Queensland (2000). He held teaching and research appointments at universities in Poland, Ireland, Australia, UK, Canada, Singapore, Hong Kong and Switzerland. At present, he is a tenured Chair Professor in the School of Information Technology and Electrical Engineering at the University of Queensland. His research interests include technologies and signal processing techniques for smart antennas and MIMO systems, low profile antennas for reception of satellite broadcast TV programs, conventional and spatial power combining techniques, six-port vector network analysers, and medical and industrial applications of microwaves. He has published over 500 technical papers, several book chapters and one book. His contributions earned him the IEEE Fellow award in 2002.